

Synergy-based Hand Pose Sensing: Reconstruction Enhancement*

Matteo Bianchi,[†] Paolo Salaris,[†] Antonio Bicchi[‡]

Abstract

Many applications in human-machine interfaces, information visualization, rehabilitation and entertainment are calling for hand pose reconstruction systems that are both accurate and economic. Unfortunately, economically and ergonomically viable sensing gloves provide limited precision due to imperfect and incomplete correspondence of sensing models with the anatomical degrees-of-freedom of the human hand, and because of measurement noise. This paper examines the problem of optimally estimating the posture of a human hand using non-ideal sensing gloves. The main idea is to maximize their performance by exploiting knowledge on how humans most frequently use their hands. To increase the accuracy of pose reconstruction without modifying the glove hardware — hence basically at no extra cost — we propose to collect, organize, and exploit information on the probabilistic distribution of human hand poses in common tasks. We discuss how a database of such an *a priori* information can be built, represented in a hierarchy of correlation patterns or *postural synergies*, and fused with glove data in a consistent way, so as to provide a good hand pose reconstruction in spite of insufficient and inaccurate sensing data. Simulations and experiments on a low-cost glove are reported which demonstrate the effectiveness of the proposed techniques.

1 Introduction

The estimation of hand pose is an enabling technology for many applications in diverse fields, ranging from human-machine interfaces to computer-aided motion analysis, virtual reality, musical performance, video games, teleoperation, robotics, and rehabilitation. Hand Pose Reconstruction (HPR) systems that prevail in the literature can be grouped in remote, or visual-based, systems and wearable, or glove-based, systems ([Sturman and Zeltzer, 1994, Dipietro et al., 2008]). All HPR methods are inherently affected by non-idealities which limit their performance: indeed, the complexity of the

*This work is supported by the European Commission under CP grant no. 248587, “THE Hand Embodied”, within the FP7-ICT-2009-4-2-1 program “Cognitive Systems and Robotics” and the ERC Advanced Grant no. 291166 “SoftHands”: “A Theory of Soft Synergies for a New Generation of Artificial Hands”.

[†]The Interdept. Research Center “Enrico Piaggio”, University of Pisa, Largo Lucio Lazzarino 1, 56100 Pisa, Italy. m.bianchi, p.salaris, bicchi@centropiaggio.unipi.it

[‡]Department of Advanced Robotics, Istituto Italiano di Tecnologia, via Morego, 30, 16163 Genova, Italy

human hand biomechanics and its variability across subjects is such that the measurement and even the mere geometric description of all its kinematic degrees of freedom is a formidable task. As a consequence, the correspondence of measurements taken by an HPR system with the anatomical Degrees-of-Freedom (DoF) of the human hand is unavoidably incomplete and imperfect. What an HPR system really provides is a set of (noisy) measurements of quantities that are related to the configuration of (some of) the hand DoF via an imperfectly known relationship.

Obviously, the intrinsic accuracy of HPR systems varies with ergonomics and cost. While visual-based HPR systems are inexpensive, non-intrusive and typically very usable, their reconstruction capabilities are as yet too low for many of the applications above mentioned. Also in glove-based HPR systems — the technology this paper focuses on — ergonomics tend to discourage the use of accurate but cumbersome sensors (such as e.g. encoders mounted on exoskeletons), and favour wearable, tissue-based devices. Economic considerations also play an important role in the choice of the technology and number of sensors. For example, the CyberGlove (CyberGlove System LLC, San Jose, CA – USA), one of the most popular glove-based systems, can come equipped with 18 or 22 piezoresistive sensors at an overall cost of 12,297 USD or 17,795 USD (2010 quotes). With the aim of enabling mass diffusion of HPR systems, more economic devices have been produced. Early devices such as e.g. Mattel's PowerGlove (Mattel Inc., El Segundo, CA–USA), which used conductive-ink sensors providing a measurement of overall finger flexion per finger for four fingers, met with scarce acceptance due to its imprecision. Recent work in the same direction is undergoing (see e.g. [Tognetti et al., 2006], HumanGlove by Humanware s.r.l., Pisa–Italy, and the survey [Dipietro et al., 2008]), which might be strongly encouraged by the availability of better reconstruction methods and software.

This paper examines the problem of optimally estimating the posture of a human hand from incomplete and imperfect glove data, improving their accuracy without modifying the hardware — hence basically at no extra cost – but rather choosing the “most likely” hand pose. The basic idea is to exploit the fact that human hands, although very complex and possibly different in size and shape, share many commonalities in how they are shaped and used in frequent everyday tasks.

Indeed, in recent years numerous studies have inquired in how the brain can organize the huge sensory-motor complexity of the human hand, with particular reference to grasping. It was shown that individuated finger motions were phylogenetically superimposed on basic grasping movements [Gordon, 2001]. It is possible to individuate a reduced number of coordination patterns, which correlate both joint motions and force exertions of multiple fingers [Schieber and Santello, 2004]. Coordination patterns in hand postures were analyzed by means of multivariate statistical methods over a grasping data set, revealing that a limited amount of so-called *principal components* (also referred to as *synergies*, or *eigenpostures* ([Mason et al., 2001])), are sufficient to explain a great part of hand pose variability. These correlation patterns can be related to both biomechanical factors [Fahrer, 1981] and synchronization between different neural motor units [Kilbreath and Gandevia, 2002]. In addition, a gradient in synergies was identified [Santello et al., 1998], showing that lower order synergies take into account covariation patterns for metacarpophalangeal (MCP) and interphalangeal (IP) joints, which are mainly responsible for coarse hand opening and closing, while higher

order synergies are used for fine hand shape adjustments.

These studies and results on human hand in grasping tasks suggest that there exist some inner hand representations of increasing complexity, which allow to reduce the number of DoFs to be used according to the desired level of approximation. From a *controllability* point of view, this idea was then adopted in robotics to define simplified approaches for the design and control of artificial hands [Brown and Asada, 2007, Gabbicini et al., 2011, Catalano et al., 2012]. On the other hand, from the *observability* point of view, this fact also suggests that it is possible to reduce the number of independent DoFs to be measured in order to obtain the hand pose estimation for a given level of approximation (cf. [Mulatto et al., 2010] for an application in hand avatar animation).

The objective of this paper, partly based on [Bianchi et al., 2012b], is to provide a hand pose estimation technique based on Bayes' inference, to exploit the knowledge on how humans most frequently use their hands. Two different approaches are followed to achieve this goal. The first one solves a constrained optimization problem of multinormal probability density function (pdf), and is mainly suited when accurately measured data are available. The second approach deals with noisy data and relies on classic Minimum Variance Estimation (MVE) techniques.

As compared to our essentially Bayesian approach, other techniques for the use of priors could be applied to pose estimation, e.g. "nearest neighbor" or "nearest neighbor blending" searches [Wang and Popović, 2009, Athitsos and Sclarof, 2003, Athitsos et al., 2004]. These methods typically apply to large databases obtained in visual-based HPR. Although their reconstruction precision can be similar to Bayesian approaches under some conditions ([Bhatia and Vandana, 2010]), these methods do not allow for systematic consideration of measurement noise in the estimation process (i.e. in deciding how much the reconstructed pose should lean towards the current measurements vs. *a priori* information). Moreover, their effectiveness is strongly dependent on the size and sampling distribution of the database, on the presence of outliers, and on heuristic rules for tuning several parameters (such as the similarity metrics and the number of "neighbors" considered [Wang and Popović, 2009]). Finally, the lack of a firm theoretical understanding of the statistical properties of the method prevents their use to define optimal design strategies of sensing devices as we propose in [Bianchi et al., 2012a], which is based on the Bayesian method below described.

To validate our method we consider experimental measurements from a set of postures acquired with a low-cost sensing glove and compare the achieved hand pose reconstruction with ground-truth measurements provided by a much more accurate optical tracking system. Statistical analyses of both experimental and simulation results demonstrate the effectiveness of the proposed procedures.

2 The hand posture estimation algorithm

Let us consider a set of measures $y \in \mathbb{R}^m$ given by a sensing glove. By using a n degree of freedom kinematic hand model, we shall assume a linear relationship between joint

variables $x \in \mathbb{R}^n$ and measurements y given by

$$y = Hx + v, \quad (1)$$

where $H \in \mathbb{R}^{m \times n}$ ($m < n$) is a full rank matrix which represents the relationship between measures and joint angles, and $v \in \mathbb{R}^m$ is a vector of measurement noise which has zero mean and Gaussian distribution with covariance matrix R . The goal is to determine the hand posture, i.e. the joint angles x , by using a set of measures y whose number is lower than the number of DoFs describing the kinematic hand model in use.

It is important to note that the model (1) may not be a good approximation for all HPR designs. Nonetheless, as we will show in Section 5, the model and the estimation procedure we use in this paper still lead to accurate results also for the glove described in [Tognetti et al., 2006] where non linearity and hysteresis affects the sensing elements.

Equation (1) represents a system where there are fewer equations than unknowns and hence is compatible with an infinite number of solutions, described e.g. as

$$x = H^\dagger y + N_h \xi, \quad (2)$$

where H^\dagger is the pseudo-inverse of matrix H , N_h is the null space basis of matrix H and $\xi \in \mathbb{R}^{(n-m)}$ is a free vector of parameters. Among these possible solutions, the least-squared solution resulting from the pseudo-inverse of matrix H (i.e. $H^\dagger = H^T (HH^T)^{-1}$) for system (1) is a vector of minimum Euclidean norm given by

$$\hat{x} = H^\dagger y. \quad (3)$$

Hereafter, we refer to equation (3) as *Pinv* method. However, the hand pose reconstruction resulting from (3) can be very far from the real one. The purpose of this paper is to improve on the accuracy of the pose reconstruction, choosing, among the possible solution to (2), the “most likely” hand pose. The basic idea is to exploit the *a priori* information obtained by collecting a large number N of grasp postures x_i , consisting of n DoFs, into a matrix $X \in \mathbb{R}^{n \times N}$. This information can be summarized in a covariance matrix $P_o \in \mathbb{R}^{n \times n}$, which is a symmetric matrix computed as

$$P_o = \frac{(X - \bar{x})(X - \bar{x})^T}{N - 1},$$

where \bar{x} is a matrix $n \times N$ whose columns contain the mean values for each joint angle arranged in vector $\mu_o \in \mathbb{R}^n$.

2.1 Probability Density Function Maximization

In this section, we initially consider the case that measurement noise is negligible. The hand pose estimation can be improved w.r.t. that obtained by (3), by exploiting the *a priori* information, that we will assume to be a multivariate normal distribution, on a set of grasping poses built beforehand and embedded in the covariance matrix P_o . The best estimation of the hand posture is given by choosing as optimality criterion

the maximization of the *probability density function* (pdf) of a multivariate normal distribution, expressed by ([Tarantola, 2005])

$$f(x) = \frac{1}{\sqrt{2\pi\|P_o\|}} \exp \left\{ -\frac{1}{2}(x - \mu_o)^T P_o^{-1} (x - \mu_o) \right\}. \quad (4)$$

This is equivalent to solving the following optimal problem:

$$\begin{cases} \hat{x} = \arg \min_{\hat{x}} \frac{1}{2}(x - \mu_o)^T P_o^{-1} (x - \mu_o) \\ \text{Subject to } y = Hx. \end{cases} \quad (5)$$

It is interesting to give a geometrical interpretation of the cost function in (5), which expresses the square of the Mahalanobis distance [Mahalanobis, 1936]. The concept of Mahalanobis distance, which takes into account data covariance structure, is widely exploited in statistics, e.g. in PC Analysis, mainly for outlier detection [Hawkins, 1980]. Accordingly, to assess if a test point belongs to a known data set, whose distribution defines an hyper-ellipsoid, we take into account both its closeness to the centroid of data set and the direction of the test point w.r.t. the centroid itself. In other words, the more samples are distributed along this direction, the more probably the test point belongs to the data set even if it is further from the center.

Taking into account (2), the optimal problem defined in (5) becomes

$$\begin{cases} \hat{\xi} = \arg \min_{\hat{\xi}} (H^\dagger y + N_h \hat{\xi} - \mu_o)^T P_o^{-1} (H^\dagger y + N_h \hat{\xi} - \mu_o) \\ \text{Subject to } y = Hx. \end{cases} \quad (6)$$

By using classic optimization procedures we obtain $\hat{\xi} = (N_h^T P_o^{-1} N_h)^{-1} N_h^T P_o^{-1} (\mu_o - H^\dagger y)$ and, substituting in (2), after some algebras, the estimation of the hand joint angles is

$$\begin{aligned} \hat{x} = [I - N_h(N_h^T P_o^{-1} N_h)^{-1} N_h^T P_o^{-1}] H^\dagger y + \\ + N_h(N_h^T P_o^{-1} N_h)^{-1} N_h^T P_o^{-1} \mu_o. \end{aligned} \quad (7)$$

Problem (5) can be also solved through the method of Lagrange multipliers. Introduce a new variable $\lambda \in \mathbb{R}^m$ and consider

$$L = \frac{1}{2}(x - \mu_o)^T P_o^{-1} (x - \mu_o) + \lambda^T (Hx - y). \quad (8)$$

By imposing $\frac{\partial L}{\partial x} = \frac{\partial L}{\partial \lambda} = 0$, we have

$$\hat{x} = \mu_o - P_o H^T (H P_o H^T)^{-1} (H \mu_o - y). \quad (9)$$

This solution can be easily shown to be equivalent to (7).

Finally, it is interesting to observe that the least-squared and pdf maximization methods have a direct application in case of each measure corresponds to a only single-DoF. In this case, H is a selection matrix whose rows are vectors of the canonical basis

in \mathbb{R}^n and the least-squared solution is simply given as $\hat{x} = H^T y$. In order to improve the hand pose reconstruction by the *a priori* information, it is possible to easily maximize $E[x|y]$ in terms of multinormal conditional distribution [Hardle and Simar, 2007]. Indeed, vector y defines a precise subset of the state variables, being X_1 , whose values are known by means of the measurement process, while X_2 indicates the rest of state variables to be estimated. This definition allows to partition the *a priori* covariance matrix as

$$\begin{pmatrix} X_1 \\ X_2 \end{pmatrix} \implies P_o = \begin{pmatrix} P_{o11} & P_{o12} \\ P_{o21} & P_{o22} \end{pmatrix} \quad (10)$$

as well as the *a priori* mean $\mu_o = (\mu_{o1} | \mu_{o2})$. The estimation of X_2 is easily derived as

$$\hat{X}_2 = E[X_2 | X_1 = y] = \mu_{o2} + P_{o21} P_{o11}^{-1} (y - \mu_{o1}). \quad (11)$$

2.2 Minimum Variance Estimation

Results in previous section are valid in the condition of $v \approx 0$. When noise is not negligible, the role of *a priori* is more emphasized.

In this section we propose an algorithm based on the Minimum Variance Estimation (MVE) technique. This method minimizes a cost functional which expresses the weighted Euclidean norm of deviations, i.e. cost functional $J = \int_X (\hat{x} - x)^T S (\hat{x} - x) p(x|z) dx$, where S is an arbitrary, semidefinite positive matrix.

Under the hypothesis that v has zero mean and Gaussian distribution with covariance matrix R , we get the solution for the minimization of J as $\hat{x} = E[x|y]$, where $E[x|y]$ represents the *a posteriori* pdf expectation value. The estimation \hat{x} can be obtained as in [Gelb, 1974] by

$$\hat{x} = (P_o^{-1} + H^T R^{-1} H)^{-1} (H^T R^{-1} y + P_o^{-1} \mu_o), \quad (12)$$

where matrix $P_p = (P_o^{-1} + H^T R^{-1} H)^{-1}$ is the *a posteriori* covariance matrix, which has to be minimized to increase information about the system. This result represents a very common procedure in applied optimal estimation when there is redundant sensor information. In under-determined problems, it is only thanks to the *a priori* information, represented by P_o and μ_o , that equation (12) can be applied (indeed, $H^T R^{-1} H$ is not invertible).

When R tends to assume very small values, the solution described in equation (12) might encounter numerical problems. However, by using the Sherman-Morrison-Woodbury formulae,

$$(P_o^{-1} + H^T R^{-1} H)^{-1} = P_o - P_o H^T (H P_o H^T + R)^{-1} H P_o \quad (13)$$

$$(P_o^{-1} + H^T R^{-1} H)^{-1} H^T R^{-1} = P_o H^T (H P_o H^T + R)^{-1}, \quad (14)$$

equation (12) can be rewritten as

$$\hat{x} = \mu_o - P_o H^T (H P_o H^T + R)^{-1} (H \mu_o - y), \quad (15)$$

and the *a posteriori* covariance matrix becomes $P_p = P_o - P_o H^T (H P_o H^T + R)^{-1} H P_o$ (cf. (13)). Hereafter, we refer to equation (15) as *MVE* method. By placing $R = 0$

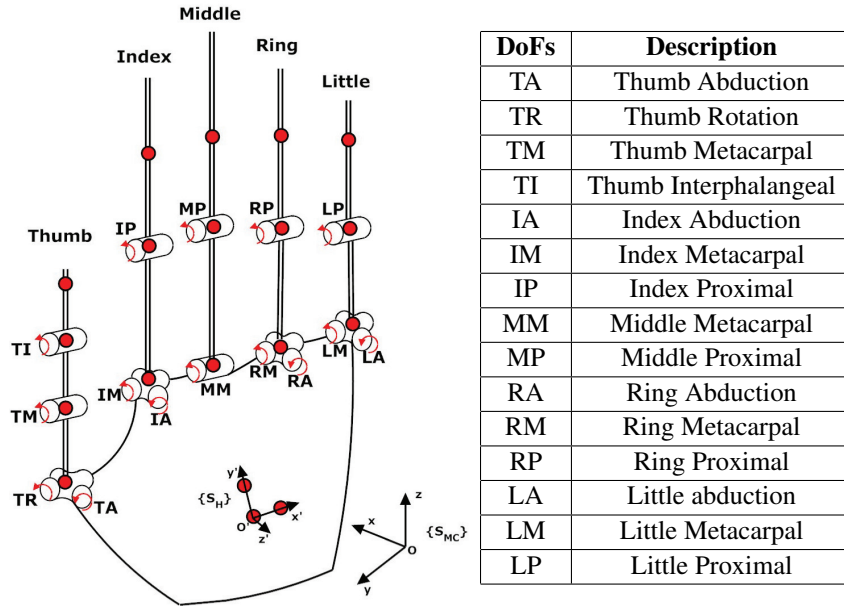


Figure 1: Kinematic model of the hand with 15 DoFs.

in (15), we obtain equation (9) and the *a posteriori* covariance matrix becomes

$$P_p = P_o - P_o H^T (H P_o H^T)^{-1} H P_o. \quad (16)$$

Notice that probability density function maximization approach is a particular case of the here described MVE technique. For this reason in the following sections we will always refer to the reconstruction technique as MVE for both noise-free and noisy measures and we will use (15) with $R = 0$ or $R \neq 0$, respectively.

3 Model and Data capture

Without loss of generality, for hand pose reconstruction we adopt the 15 DoFs model reported in figure 1, also used in [Santello et al., 1998, Gabiccini et al., 2011]. The model DoFs are: 4 DoFs for the thumb, i.e. TR, TA, TM, TI (Thumb Rotation, Abduction, Metacarpal, Interphalangeal); 3 DoFs for the index, i.e. IA, IM, IP (Index Abduction, Metacarpal, Proximal interphalangeal); 2 DoFs for the middle, i.e. MM, MP (Middle Metacarpal, Proximal interphalangeal); 3 DoFs for the ring, i.e. RA, RM, RP (Ring Abduction, Metacarpal, Proximal interphalangeal); 3 DoFs for the little, i.e. LA, LM, LP (Little Abduction, Metacarpal, Proximal interphalangeal). Notice that, the middle finger has no abduction since it is considered the “reference finger” in the sagittal plane of the hand.

A large number of static grasp positions were collected using 19 active markers and an optical motion capture system (Phase Space Inc., San Leandro, CA - USA). More

specifically, all the grasps of the 57 imagined objects described in [Santello et al., 1998] were performed twice by subject AT (M,26), in order to define a set of 114 *a priori data*. Moreover, in a separated set of experiments, 54 grasp poses of a wide range of different imagined objects, only partly overlapping, were executed by a different subject LC (M,26)¹ (hereafter, we refer to this set as the *validation data*). Validation data consist of two parts acquired in parallel for each posture, consisting of 1) the measurements from sensing glove used in Section 5 (*test data*), and 2) the Phase Space data, which is then used as “ground truth”.

Phase Space acquisitions from *validation data* are also used to simulate a glove as described in Section 4. According to the number of measures, we have considered from the postures in this set only some joints, assuming to select them individually based on the non-zero elements in the measurement matrix (*simulation data*). Different algorithms are validated by applying them to the same test and simulation data, and comparing the results with ground truth data.

Indeed, we can consider the processed hand poses acquired with Phase Space as a good approximation of real hand positions, given the high accuracy provided by this optical system to detect markers (the amount of static marker jitter is inferior than 0.5 mm, usually 0.1 mm) and assuming a linear correlation (due to skin stretch) between marker motion around the axes of rotation of the joint and the movement of the joint itself [Zhang et al., 2003]. Of course, even if the glove cloth exhibits elastic properties, individuals with very different hand dimensions and shapes w.r.t. glove footprint may affect the experimental outcomes. For this reason, in our experiment, we chose subject whose hand shape adapts very well to the glove used, and hence, the above assumption is still reasonable. None of the subjects had physical limitations that would affect the experimental outcomes. Data collection from subjects in this study was approved by the University of Pisa Institutional Review Board. Markers were placed on the



Figure 2: The sensing glove (on the left) and sensing glove with added markers (on the right).

glove in correspondence of the joints referring to [Fu and Santello, 2010], see figure 2. Four markers were used for the thumb and three markers for each of the rest of the fingers. Additional three markers placed on the dorsal surface of the palm defines a local reference system S_H . Markers were sampled at 480 Hz and their positions are

¹These hand posture acquisitions are available at <http://handcorpus.org/>

given referring to the global reference system S_{MC} , as it is defined during the calibration phase of the acquisition system (cf. figure 1).

Based on marker positions obtained by the Phase Space system, w.r.t. S_H , joint angles are computed by means the *ikine* function of Matlab Kinematic Toolbox. This function implements an iterative algorithm of kinematic inversion, which has been suitably modified by adapting computational tolerance to guarantee numerical convergence. A moving average filter is exploited for data pre-filtering, thus enhancing Signal Noise Ratio (SNR). As a preliminary phase, the hand is posed in a reference position, where fingers flexion-extension is nearly zero, and phalanx length and eventual offset angles are computed.

Normality assumption on the acquired *a priori* set is tested by means of a Q-Q plot-based graphical method for multidimensional variables [Chambers et al., 1983, Holgersson, 2006]. The quantile plot is usually obtained by plotting the ordered estimated Mahalanobis measures against the chi-square distribution quantiles. If normality is met, the graph should display a fairly straight line on the diagonal (i.e. 45° slope line). In our case, the linear fitting with straight 45° slope line provides an adjusted r-squared coefficient of 0.6. This result suggests that the normality assumption is reasonable even if not fully met. However, the Gauss-Markov theorem [Rao, 1973] ensures, that the MVE is the Best Linear Unbiased Estimator (BLUE) in the minimum-variance sense even for non-Gaussian *a priori* distributions [Bicchi and Canepa, 1994]. In addition, central limit theorem [Hardle and Simar, 2007] can guarantee, to some extents, the application of MVE method to cases that depart from the strict linear-Gaussian hypothesis for *a priori* distribution (and noise distribution as well).

4 Simulation Results

Without loss of generality, we simulate an ideal glove which is able to measure only metacarpal joints, i.e. TM, IM, MM, RM and LM (see figure 1), by using the acquisitions obtained with Phase Space (*simulation data*). Notice that, any other choice and number of measured joints would be effective in order to validate our methods. The measurement matrix for this simulated glove will be referred as H_s . An additional random Gaussian noise with standard deviation of 7° is considered on each measurement. This value is chosen in a cautionary manner, based on data about common technologies and tools used to measure hand joint positions [Simone et al., 2007]. More specifically, this value expresses the reliability threshold of manual goniometry with skilled therapists in measures for rehabilitation procedures [Wise et al., 1990].

The estimation performance is evaluated in terms of estimation errors. Pose estimation errors (i.e. the mean of DoF absolute estimation errors computed for each pose $e_i = \frac{1}{n} \sum_{i=1}^n |x_i - \hat{x}_i|$), and DoF absolute estimation errors are considered and averaged over all the number of reconstructed poses. We perform these two types of analysis in order to furnish a more clear result comprehension. Indeed, pose estimation errors provide an useful but only global indication about the technique outcomes, potentially leading to some biased observations. For example, we might obtain a hand pose reconstruction with all the fingers in a position the same average error of a hand pose reconstruction with all the fingers but one in the real position and the one misposi-

tioned very distant from the real one. Therefore, to overcome this limitation we also analyze each DoF estimation accuracy. In addition, some reconstructed poses are displayed w.r.t. the reference ones, to provide a qualitative representation mainly focused on reconstruction *likelihood* exhibited by reconstructed poses with common grasp postures. Statistical differences between estimated pose and joint errors obtained with above described techniques are computed by using classic tools, after having tested for normality and homogeneity of variances assumption on samples (through Lilliefors' composite goodness-of-fit test and Levene's test, respectively). Standard two-tailed t-test (hereinafter referred as T_{eq}) is used in case of both the assumptions are met, a modified two-tailed T-test is exploited (Behrens-Fisher problem, using Satterthwaite's approximation for the effective degrees of freedom, hereinafter referred as T_{neq}) when variance assumption is not verified and finally a non parametric test is adopted for the comparison (Mann-Whitney U-test, hereinafter referred as U) when normality hypothesis fails. Significance level of 5% is assumed and p-values less than 10^{-4} are posed equal to zero.

In case of noise-free measurements, mean absolute pose error obtained with MVE is $6.69 \pm 2.38^\circ$, while with Pinv it is equal to $13.89 \pm 3.09^\circ$, with observed statistical difference between the two methods ($p \simeq 0$, T_{eq}). What is noticeable is that MVE provides a better pose estimate than the one obtained using Pinv in terms of both mean pose absolute estimate error and considering maximum absolute pose estimation error (MVE: 13.18° vs. Pinv: 20.82°).

In case of noisy measurements, mean absolute pose estimation error with MVE is $8.52 \pm 2.86^\circ$, while with Pinv we get $15.71 \pm 3.08^\circ$. Also in this case statistical difference is observed between MVE and Pinv ($p \simeq 0$, T_{neq}). Notice that MVE still provides the best pose estimate and the smallest pose absolute maximum error (MVE: 17.14° vs. Pinv: 23.39°).

In table 1 absolute average estimation errors for each DoF with their corresponding standard deviations are reported for MVE and Pinv procedures. Noise-free measures are considered. Significant statistical differences between the two techniques are found considering estimation errors for all DoFs, except for those directly measured and for TA and TI. MVE exhibits an estimation performance in terms of mean error which is better, or not statistically significantly different, than the one achieved by Pinv, except for the IA DoF; however the difference between the mean errors for the two methods is the smallest (less than 6°) among all the differences computed for the significantly different estimated DoFs. MVE provides the smallest maximum errors except for the IA DoF; however the difference with maximum error obtained using Pinv is less than 12° . It is hard to determine why the Pinv method seem to give better estimates w.r.t. the MVE for this joint, but this effect certainly depends on the poses to be reconstructed. Notice that the IA joint is not directly measured, so that the Pinv method always estimates this DoF to be zero. In table 2 values of each DoF estimation absolute error averaged over all poses, with their corresponding standard deviations, are reported in case of noise. Maximum errors are calculated and statistical significance in result comparison for each DoF estimation, between the aforementioned techniques, is indicated in table 2. Notice that MVE furnishes the best performance with average estimation errors which are always inferior or not statistically different from the ones obtained using Pinv algorithm, except for IA DoF for which Pinv produces the smallest average

| DoF | Mean±Std | | Max Error | | p-values |
|------------|------------|-------------|-----------|-------|---------------|
| | MVE | Pinv | MVE | Pinv | |
| TA | 10.74±8.45 | 14.04±11.10 | 31.65 | 32.74 | 0.1794 |
| TR | 7.16±4.54 | 27.62±10.24 | 19.50 | 45.65 | 0 |
| TM* | 0 | 0 | 0 | 0 | – |
| TI | 4.81±3.68 | 6.74±5.54 | 19.69 | 23.16 | 0.1179 |
| IA | 11.96±5.33 | 6.27±3.27 | 26.35 | 14.90 | 0 |
| IM* | 0 | 0 | 0 | 0 | – |
| IP | 13.26±7.06 | 28.87±13.79 | 27.46 | 59.41 | 0 |
| MM* | 0 | 0 | 0 | 0 | – |
| MP | 12.35±7.75 | 29.84±13.64 | 29.94 | 57.78 | 0 |
| RA | 3.45±2.43 | 10.17±3.78 | 9.51 | 16.45 | 0 |
| RM* | 0 | 0 | 0 | 0 | – |
| RP | 13.40±9.65 | 34±13.88 | 39.33 | 65.43 | 0 |
| LA | 11.33±5.87 | 24.28±5.18 | 24.47 | 37.89 | 0 ◊ |
| LM* | 0 | 0 | 0 | 0 | – |
| LP | 11.94±9.50 | 26.50±13.65 | 26.58 | 63.64 | 0 |



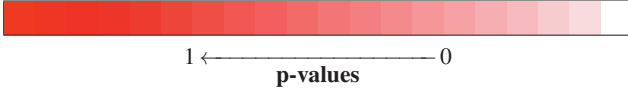
1 ←————— 0
p-values

* indicates a measured DoF.

Table 1: Average estimation errors and standard deviations for each DoF [°] for the simulated acquisitions without noise. MVE and Pinv methods are considered. Maximum errors are also reported as well as p-values from the evaluation of DoF estimation errors between MVE and Pinv. A color map describing p-values is also added to simplify result visualization. ◊ indicates that T_{eq} test is exploited for the comparison. ‡ indicates a T_{neq} test. When no symbol appears near the tabulated values, it means that U test is used. **Bold** value indicates no statistical difference between the two methods under analysis at 5% significance level. When the difference is significant, values are reported with a 10^{-4} precision. p-values less than 10^{-4} are considered equal to zero.

estimation error. However, the difference between IA mean errors calculated with the two procedures is less than 3° . No statistically significant difference are found between MVE and Pinv for TI, IM, MM, RM and LM DoFs. It is interesting to notice that the MVE method seems to give more accurate estimates for certain DoFs (e.g. TA, RA, LA) with noise than without noise even if in the latter case, the average absolute pose estimation error is the smallest one. The solution obtained by this method depends on different factors: the measured joint angles, the *a priori* covariance matrix (in particular how joint variables covary with each other) and the amplitude and the structure of the measurement noise. How these factors interact to determine the estimation is hard to describe, especially for large dimension problems. Indeed, increasing noise, MVE tends to disregard the information provided by the measurement process and to pro-

| DoF | Mean±Std | | Max Error | | p-values |
|------------|-------------|-------------|-----------|-------|-------------|
| | MVE | Pinv | MVE | Pinv | |
| TA | 8.93±6.64 | 14.04±11.10 | 31.12 | 32.74 | 0.0496 ‡ |
| TR | 8.10±5.66 | 27.62±10.24 | 22.53 | 45.65 | 0 |
| TM* | 2.96±2.16 | 5.62±4.25 | 8.25 | 17.01 | 0.0009 |
| TI | 6.80±4.95 | 6.74±5.54 | 20.10 | 23.16 | 0.66 |
| IA | 10.69±5.50 | 6.27±3.27 | 25.45 | 14.90 | 0 |
| IM* | 4.21±3.24 | 5.40±3.57 | 13.71 | 13.86 | 0.07 |
| IP | 14.63±7.86 | 28.87±13.79 | 34.16 | 59.41 | 0 |
| MM* | 4.80±2.74 | 5.23±3.97 | 10.35 | 20.03 | 0.95 |
| MP | 13.87±8.39 | 29.84±13.64 | 38.19 | 57.78 | 0 |
| RA | 3.13±2.18 | 10.17±3.78 | 9.00 | 16.45 | 0 |
| RM* | 4.62±3.42 | 5.28±3.73 | 13.75 | 17.56 | 0.34 ◊ |
| RP | 16.98±11.47 | 34.00±13.88 | 50.58 | 65.43 | 0 |
| LA | 8.99±5.16 | 24.28±5.18 | 20.44 | 37.89 | 0 ◊ |
| LM* | 4.27±3.14 | 5.78±4.30 | 15.47 | 18.71 | 0.09 |
| LP | 14.89±9.95 | 26.50±13.65 | 48.10 | 63.64 | 0 ‡ |



1 ←—————→ 0
p-values

* indicates a measured DoF.

Table 2: Average estimation errors and standard deviations for each DoF [°] for the simulated acquisitions with noise. MVE and Pinv methods are considered. Maximum errors are also reported as well as p-values from the evaluation of DoF estimation errors between MVE and Pinv. A color map describing p-values is also added to simplify result visualization. ◊ indicates that T_{eq} test is exploited for the comparison. ‡ indicates a T_{neq} test. When no symbol appears near the tabulated values, it means that U test is used. **Bold** value indicates no statistical difference between the two methods under analysis at 5% significance level. When the difference is significant, values are reported with a 10^{-4} precision. p-values less than 10^{-4} are considered equal to zero.

vide joint angle estimates which are closer to the *a priori* mean μ_o , in a fashion which depends on the level of noise and on how much the measured joints are correlated with the other ones.

It should be noticed that the MVE method guarantees that the mean squared norm of the joint error vector (i.e. the Mean Squared Error, $MSE = \frac{1}{N} \sum_{i=1}^N \|\hat{x} - x\|^2$, where N represents the number of predictions) is minimized, but not necessarily the value of each single component. Same applies with noise: indeed, some particular joints have a lower error with noise than without noise, yet the overall error norm (across all joints) is always higher if noise is present. Indeed, if the joint angles of both the estimations and the reference poses are in degrees, the MSE with the MVE method (Pinv method) is 1583 (6367) in case of noise-free measures and 1992 (6634) in case of noise, hence

it increases with noise. The fact that noise happens to reduce the error in some joints is a statistically insignificant case, that has occurred with the validation set reported in the paper. Using other validation sets, we have obtained estimates where noise reduces the error of different individual joints, or increases all components: however, as theory predicts, the overall mean square error vector is always increased by noise. The whole argument rests on the fact that the validation sets are samples from the same distribution, of which the *a priori* set is assumed to provide a statistically accurate description.

It could also be noticed that the Pinv method exhibits the same errors for non-measured joints with and without noise. As explained in Section 4, in case of a selection matrix H_s , the Pinv solution is simply given by $\hat{x} = H_s^T y$ (i.e. $H_s^\dagger = H_s^T$). As a consequence, for both noisy and noise-free measurements, the minimum Euclidean norm solution \hat{x} has zero values for all non-measured components of \hat{x} , while noise only affects the measured ones.

In figure 3 some reconstructed poses are displayed in comparison with their corresponding reference values achieved with Phase Space System, with and without noise. Notice that MVE qualitatively shows the best reconstruction results, thus maintaining, unlike Pinv, the likelihood with common grasping poses because of the *a priori* information.

5 Experimental Results

We test for the effectiveness of our reconstruction procedure using a sensorized glove based on Conductive Elastomer (CE). CE strips are printed on a Lycra[®]/cotton fabric in order to follow the contour of the hand, see figure 2. Connection to 20 different sensor segments of the polymeric strip is realized using additional conductive elastomer elements printed on the dorsal side of the glove [Tognetti et al., 2006].

Since CE materials present piezoresistive characteristics, sensor elements corresponding to different segments of the contour of the hand length change as the hand moves. These movements cause variations in the electrical properties of the material, which can be revealed by reading the voltage drop across such segments. The sensors are connected in series thus forming a single sensor line while the connections intersect the sensor line in the appropriate points. An *ad hoc* electronic front-end was designed to compensate the resistance variation of the connections, made by the same material of the sensors, using an high input impedance stage.

Data coming from the front-end is then low pass filtered, digitalized and acquired by means of a general purpose DAQ card, and finally elaborated on a computer.

Data processing is based on the assumption that changes in the electrical characteristics of the sensor elements, corresponding to different segments of the contour of the hand, are mainly associated with changes in the angle of the joint such sensor elements cut across. Furthermore, it was assumed that the hand aperture linearly relates to changes in the electrical characteristics of the sensor elements occurring as joint angles change [Lorussi et al., 2004, Tognetti et al., 2007, Tognetti et al., 2008].

This sensorized glove represents one of the most recent and inexpensive technical solutions in glove device literature. However, it is limited by some factors, e.g. cloth

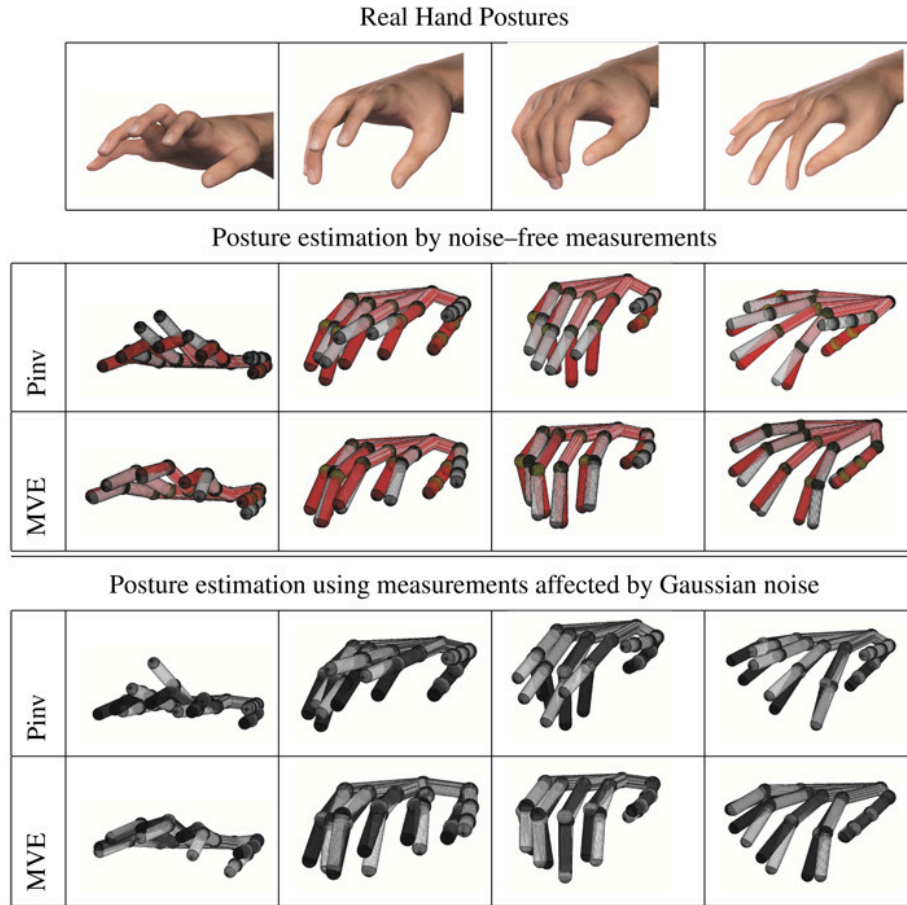


Figure 3: Hand pose reconstructions with Pinv and MVE algorithms by using a selection matrix H_s which allows to measure TM, IM, MM, RM and LM (see figure 1). In color the “real” hand posture whereas in white the estimated one.

support which affects measurement repeatability as well as hysteresis and non linearities due to piezoresistive material properties. Moreover, the assumptions done for data processing (the relationship between joint angle and sensors as well the linearity between hand aperture and electrical property changes) can act like potential sources of errors.

In order to obtain an estimation of the measurement matrix of the glove H_g , a calibration phase was performed by using a number N of poses from *validation data*. This number has to be larger or equal than the dimension of the state to estimate, i.e. $N \geq 15$. $X_g \in \mathbb{R}^{15 \times 15}$ collects “ground truth”, while matrix $Y_g \in \mathbb{R}^{5 \times 15}$ organizes the measures from the glove (*test data*). These measures represent the values of the

signals referred to measured joints of static postures, averaged over the last 50 acquired samples equally spaced on a period of 5 s. For the acquisition, a DAQ card which works at 250 kS/s (NI PCI-6024E by National Instruments, Austin, Texas, USA) has been used within Matlab Simulink[®] environment.

An estimation \hat{H}_g of the measurement matrix can be obtained by using the relation $Y_g = \hat{H}_g X_g$ as

$$\hat{H}_g = Y_g ((X_g^T)^\dagger)^T. \quad (17)$$

What is noticeable from the calibration outcomes is that the sensing glove provides five measurements, each related to a weighted sum of several joint angles (according to weights in the corresponding row of \hat{H}_g matrix).

In literature there are several methods and tools to calibrate datagloves for capturing motion of human hand, which depend on the particular design of the sensing devices (e.g. [Jin et al., 2010, Wang and Dai, 2009]). A common procedure for calibration is to place subject's hand in known configurations and to suitably edit parameters, such as offset, to match sensor readings with physical hand pose [Dipietro et al., 2008]. The technique we adopt is simple and it enables for an approximated estimation of the measurement matrix, which is sufficient for our purposes. Although intrinsic hysteresis and nonlinearities of glove sensing elements can not be correctly modeled independently from the adopted calibration procedure, and hence some modeling errors might occur, we show in our experiments that the hand pose estimations obtained by the proposed reconstruction methods are accurate.

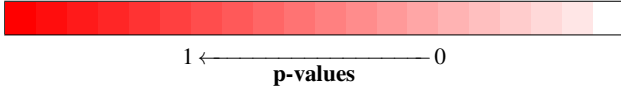
Although some modeling errors might be observed due to intrinsic non-linearities and hysteresis of glove sensing elements, we show in our experiments that the outcomes of the proposed reconstruction methods are quite robust also w.r.t. calibration procedures.

5.1 Results and Discussion

We characterize measurement noise in terms of fluctuations w.r.t. the aforementioned average values of glove measures, thus obtaining noise covariance matrix R . Noise level is less than 10% measurement amplitude.

The average absolute pose estimation error with MVE is $10.94 \pm 4.24^\circ$, while it is equal to $19.00 \pm 3.66^\circ$ by using PinV. Statistical difference is observed between the two techniques ($p = 0$, T_{eq}). Notice that MVE exhibits the best pose reconstructions also in terms of maximum errors (25.18° for MVE vs. 30.30° for PinV). Absolute average reconstruction errors for each DoF are reported in table 3. MVE produces smaller mean errors than those obtained with PinV with statistical difference, except for RA DoF, which exhibits a limited average estimation error ($\approx 6^\circ$), and TA. No statistical differences are observed also for IM, RM and LM, which exhibit high estimation error values. A possible explanation is that these DoFs present large variations in grasping tasks, and hence their values are more affected by hysteresis and non linearities. For TI the smallest average estimation is observed with PinV. IA DoF presents the smallest absolute average estimation error with PinV, although p-value from the comparisons between the two techniques for the estimation of this DoF is close to the significance threshold.

| DoF | Mean±Std | | Max Error | | p-values |
|-----------|-------------|-------------|-----------|-------|-------------|
| | MVE | Pinv | MVE | Pinv | |
| TA | 12.12±9.98 | 14.37±10.78 | 36.63 | 34.28 | 0.28 |
| TR | 9.20±7.13 | 26.46±10.49 | 26.34 | 46.43 | 0 |
| TM | 4.36±3.73 | 6.43±4.44 | 13.25 | 18.50 | 0.0093 |
| TI | 14.56±9.96 | 7.84±5.47 | 33.25 | 22.38 | 0.0008 |
| IA | 9.82±6.89 | 7.10±5.08 | 29.60 | 21.18 | 0.0381 |
| IM | 15.27±11.86 | 16.48±12.62 | 46.76 | 43.58 | 0.58 |
| IP | 9.60±7.65 | 31.47±14.70 | 27.40 | 61.11 | 0 |
| MM | 14.40±12.84 | 19.88±14.58 | 53.03 | 51.47 | 0.0232 |
| MP | 6.80±6.49 | 24.36±9.85 | 24.74 | 43.72 | 0 |
| RA | 6.20±4.31 | 5.69±4.72 | 15.72 | 20.90 | 0.51 |
| RM | 19.00±13.44 | 19.22±11.81 | 61.98 | 46.32 | 0.67 |
| RP | 8.98±8.91 | 31.51±13.98 | 32.24 | 60.62 | 0 |
| LA | 11.42±8.50 | 32.24±6.98 | 29.59 | 48.11 | 0 |
| LM | 17.37±12.51 | 17.98±11.81 | 58.40 | 45.05 | 0.26 |
| LP | 8.43±6.36 | 23.90±12.53 | 26.07 | 56.21 | 0 |



1 ←—————→ 0
p-values

Table 3: Average estimation errors and standard deviations for each DoF [°], for the sensing glove acquisitions. MVE and Pinv methods are considered. Maximum errors are also reported as well as p-values from the evaluation of DoF estimation errors between MVE and Pinv. A color map describing p-values is also added to simplify result visualization. \diamond indicates that T_{eq} test has been exploited for the comparison. \ddagger indicates a T_{neq} test. When no symbol appears near the tabulated values, it means that U test has been used. **Bold** value indicates no statistical difference between the two methods under analysis at 5% significance level. When the difference is significant, values are reported with a 10^{-4} precision. p-values less than 10^{-4} are considered equal to zero.

As previously described for absolute average reconstruction errors, maximum DoF reconstruction errors for MVE are observed especially for those measured DoFs with maximum variations in grasping tasks. This fact may be probably interpreted considering the non linearities in sensing glove elements leading to inaccurate estimation of H_g , hence to inaccurate measures.

Finally, except for some singular poses, the best estimation accuracy is provided by MVE for which a good robustness to errors in measurement process modeling is also observed. However, the latter errors have not been taken numerically into account in our analyses. Moreover, as it can be seen in figure 4, reconstructed hand configurations obtained by MVE preserve likelihood with real poses, as opposed to the Pinv algorithm.



Figure 4: Hand pose reconstructions with Pinv and MVE algorithms, with measures given by sensing glove. In color the “real” hand posture whereas in white the estimated one.

6 Conclusions

In this work reconstruction techniques to estimate static hand poses from a reduced number of measures given by an input glove-based devices are presented. These techniques are based on classic optimization and applied optimal estimation methods. The main innovation relies on the exploitation of the *a priori* information embedded in the covariance structure of a set of grasp poses. This covariance individuates some coordination patterns, defined as *postural synergies*, which reduce hand DoFs to be measured and controlled.

Simulations results, where noise effects are also considered, and experiments with a low-cost sensing glove are reported. Reconstruction accuracy is compared with the one obtained with a simple pseudo-inverse based algorithm. Statistical analyses demonstrate the effectiveness of the here proposed hand pose reconstructions.

The problem of inter-subject and gender generalizability of our method is not systematically addressed in the present work and it is deferred to future developments. However, it is worth underscoring again that our results have been obtained using *a priori* data from a different subject than the one performing validation. Furthermore, it can be observed that [Santello et al., 1998] report that principal component analyses of the same imagined grasped objects performed by male and female subjects revealed a strong degree of similarity and no gender bias was observed.

The results can be useful to improve a large class of human-interfaces in many application fields, e.g. video-games or tele-robotics, where fine hand position individuation and low-cost devices are crucial features to allow a reliable haptic experience.

In [Bianchi et al., 2012a] we apply this reconstruction procedure to the measures provided by an optimally designed sensing glove.

Acknowledgments

Authors gratefully acknowledge Alessandro Tognetti and Nicola Carbonaro for their assistance in sensing glove configuration setting and Armando Turco for his help in data acquisition with the optical tracking system.

References

- [Athitsos and Sclarof, 2003] Athitsos, V. and Sclarof, S. (2003). Estimating 3d hand pose from a cluttered image. In *In Proceedings of the IEEE Conference on Computer Vision and Pattern Recognition*, volume 2, pages 432 – 439.
- [Athitsos et al., 2004] Athitsos, V., Sclarof, S., and Kollios, G. (2004). Boostmap: A method for efficient approximate similarity rankings. In *In Proceedings of the IEEE Conference on Computer Vision and Pattern Recognition*, volume 2, pages 268 – 275.
- [Bhatia and Vandana, 2010] Bhatia, N. and Vandana (2010). Survey of nearest neighbor techniques. *International Journal of Computer Science and Information Security*, 8(2):302 – 305.
- [Bianchi et al., 2012a] Bianchi, M., Salaris, P., and Bicchi, A. (2012a). Synergy-based hand pose sensing: Optimal glove design. *The International Journal of Robotics Research*. Submitted.
- [Bianchi et al., 2012b] Bianchi, M., Salaris, P., Turco, A., Carbonaro, N., and Bicchi, A. (2012b). On the use of postural synergies to improve human hand pose reconstruction. In *IEEE Haptics Symposium*, pages 91 – 98.
- [Bicchi and Canepa, 1994] Bicchi, A. and Canepa, G. (1994). Optimal design of multivariate sensors. *Measurement Science and Technology (Institute of Physics Journal “E”)*, 5:319 – 332.
- [Brown and Asada, 2007] Brown, C. and Asada, H. (2007). Inter-finger coordination and postural synergies in robot hands via mechanical implementation of principal component analysis. In *IEEE-RAS International Conference on Intelligent Robots and Systems*, pages 2877 – 2882.
- [Catalano et al., 2012] Catalano, M., Giorgio, G., Serio, A., Farnioli, E., Piazza, C., and Bicchi, A. (2012). Adaptive synergies for a humanoid robot hand. In *2012 IEEE-RAS International Conference on Humanoid Robots*. accepted.
- [Chambers et al., 1983] Chambers, J., Cleveland, W., and Kleiner, B. (1983). *Graphical Methods for Data Analysis*. Wadsworth and Brooks/Cole, Pacific Grove, CA, USA.

- [Dipietro et al., 2008] Dipietro, L., Sabatini, A., and Dario, P. (2008). A survey of glove-based systems and their applications. *Systems, Man, and Cybernetics, Part C: Applications and Reviews, IEEE Transactions on*, 38(4):461 –482.
- [Fahrer, 1981] Fahrer, M. (1981). *The hand*, chapter Interdependent and independent actions of the fingers, pages 399 – 403. Philadelphia, PA: Saunders.
- [Fu and Santello, 2010] Fu, Q. and Santello, M. (2010). Tracking whole hand kinematics using extended kalman filter. In *Engineering in Medicine and Biology Society (EMBC), 2010 Annual International Conference of the IEEE*, pages 4606 – 4609.
- [Gabiccini et al., 2011] Gabiccini, M., Bicchi, A., Prattichizzo, D., and Malvezzi, M. (2011). On the role of hand synergies in the optimal choice of grasping forces. *Autonomous Robots [special issue on RSS2010]*, 31(2 - 3):235 – 252.
- [Gelb, 1974] Gelb, A. (1974). *Applied Optimal Estimation*. M.I.T. Press, Cambridge, US-MA.
- [Gordon, 2001] Gordon, A. (2001). *Handbook of Brain and Behaviour in Human Development*, chapter Development of hand motor control, pages 513 – 537. The Netherlands: Kluwer Academic.
- [Hardle and Simar, 2007] Hardle, W. and Simar, L. (2007). *Applied Multivariate Statistical Analysis*. Springer-Verlag Berlin Heidelberg New York.
- [Hawkins, 1980] Hawkins, D. (1980). *Identification of Outliers*. Chapman and Hall, London.
- [Holgersson, 2006] Holgersson, H. E. T. (2006). A graphical method for assessing multivariate normality. *Computational Statistics*, 21:141–149.
- [Jin et al., 2010] Jin, S., Li, Y., and Chen, W. (2010). A novel dataglove calibration method. In *Computer Science and Education (ICCSE), 2010 5th International Conference on*, pages 1825 –1829.
- [Kilbreath and Gandevia, 2002] Kilbreath, S. and Gandevia, S. (2002). Limited independent flexion of the thumb and fingers in human subjects. *J Physiol*, 543:289 – 296.
- [Lorussi et al., 2004] Lorussi, F., Rocchia, W., Scilingo, E. P., Tognetti, A., and De Rossi, D. (2004). Wearable, redundant fabric-based sensor arrays for reconstruction of body segment posture. *IEEE Sensors Journal*, 4(6):807–818.
- [Mahalanobis, 1936] Mahalanobis, P. C. (1936). On the generalised distance in statistics. *Proceedings of the National Institute of Sciences of India*, 2(1):49 – 55.
- [Mason et al., 2001] Mason, C. R., Gomez, J. E., and Ebner, T. J. (2001). Hand synergies during reach-to-grasp. *J Neurophysiol*, 86:2896 – 2910.

- [Mulatto et al., 2010] Mulatto, S., Formaglio, A., Malvezzi, M., and Prattichizzo, D. (2010). Animating a synergy-based deformable hand avatar for haptic grasping. In *International Conference EuroHaptics*, pages 203 – 210.
- [Rao, 1973] Rao, C. R. (1973). *Linear Statistical Inference and Its Applications*. Wiley, New York.
- [Santello et al., 1998] Santello, M., Flanders, M., and Soechting, J. F. (1998). Postural hand synergies for tool use. *The Journal of Neuroscience*, 18(23):10105 – 10115.
- [Schieber and Santello, 2004] Schieber, M. H. and Santello, M. (2004). Hand function: peripheral and central constraints on performance. *Journal of Applied Physiology*, 96(6):2293 – 2300.
- [Simone et al., 2007] Simone, L. K., Sundarrajan, N., Luo, X., Jia, Y., and Kamper, D. G. (2007). A low cost instrumented glove for extended monitoring and functional hand assessment. *Journal of Neuroscience Methods*, 160(2):335–348.
- [Sturman and Zeltzer, 1994] Sturman, D. J. and Zeltzer, D. (1994). A survey of glove-based input. *Computer Graphics and Applications, IEEE*, 14(1):30 – 39.
- [Tarantola, 2005] Tarantola, A. (2005). *Inverse Problem Theory and Model Parameter Estimation*. SIAM.
- [Tognetti et al., 2007] Tognetti, A., Bartalesi, R., Lorussi, F., and De Rossi, D. (2007). Body segment position reconstruction and posture classification by smart textiles. *Transaction of the Institute of Measurement and Control*, 29(3-4):215–253.
- [Tognetti et al., 2008] Tognetti, A., carbonaro, N., Dalle Mura, G., Tesconi, M., Zupone, G., and De Rossi, D. (2008). Sensing garments for body posture and gesture classification. *TUT Magazine*, 68:33–39.
- [Tognetti et al., 2006] Tognetti, A., Carbonaro, N., Zupone, G., and De Rossi, D. (2006). Characterization of a novel data glove based on textile integrated sensors. In *Annual International Conference of the IEEE Engineering in Medicine and Biology Society, EMBC06, Proceedings.*, pages 2510 – 2513.
- [Wang and Dai, 2009] Wang, B. and Dai, S. (2009). Dataglove calibration with constructed grasping gesture database. In *Virtual Environments, Human-Computer Interfaces and Measurements Systems, 2009. VECIMS '09. IEEE International Conference on*, pages 6 –11.
- [Wang and Popović, 2009] Wang, R. Y. and Popović, J. (2009). Real-time hand-tracking with a color glove. *Transaction on Graphics*, 28(3):63 – 71.
- [Wise et al., 1990] Wise, S., Gardner, W., Sabelman, E., Valainis, E., Wong, Y., Glass, K., Drace, J., and Rosen, J. M. (1990). Evaluation of a fiber optic glove for semi-automated goniometric measurements. *Journal Of Rehabilitation Research And Development*, 27(4):411–424.

[Zhang et al., 2003] Zhang, X., Lee, S., and Braido, P. (2003). Determining finger segmental centers of rotation in flexion-extension based on surface marker measurement. *Journal of Biomechanics*, 36:1097 – 1102.